Applied Surface Science 257 (2010) 1602–1606

Contents lists available at ScienceDirect

Applied Surface Science

journal homepage: www.elsevier.com/locate/apsusc

Effects of air annealing on the optical, electrical, and structural properties of nanostructured ZnS/Au/ZnS films

S.M.B. Ghorashi, A. Behjat*, M. Neghabi, G. Mirjalili

Atomic and Molecular Group, Faculty of Physics, Yazd University, Yazd, Iran

ARTICLE INFO

Article history:
Received 4 July 2010
Received in revised form 25 August 2010
Accepted 25 August 2010
Available online 9 September 2010

PACS:
44.15.Eq
78.67.Pt
78.20.Ci

Keywords:
Au film
Transparent conductive
Annealing temperature
Optical and electrical properties
XRD
SEM

ABSTRACT

In this paper, transparent conductive ZnS/Au/ZnS nano-multilayer films have been designed and the optimum thickness of gold and zinc sulfide layers are calculated. The conductive transparent ZnS/Au/ZnS nano-multilayer structure with optimized thickness have also been fabricated on a glass substrate by thermal evaporation and have been annealed in air at different temperatures. The electrical, optical and structural properties of the films such as electrical resistivity, optical transmittance, grain size have been obtained. X-ray diffraction patterns show that increase in annealing temperature increases the crystallinity of the structures. Moreover, Scanning electron microscope images of the samples show that the grain sizes become larger by increasing the annealing temperature which is in consistence with the X-ray diffraction analysis.

1. Introduction

Nowadays, transparent conducting (TC) films are used in several application, including flat panel displays [1], energy-efficient windows [2,3], thin film transistors [4], gas sensors [5], organic solar cells [6,7] and organic light emitting diodes [8]. These films have inimitable characteristics such as low resistivity, high optical transmission in the visible spectrum and high absorption in ultraviolet (UV) and infra-red (IR) region [2,3,9,10]. The problems such as complex production processes at high temperatures for some of transparent conducting oxide (TCO) films do not exist during TCs process [11,12]. Dielectric/metal/dielectric (D/M/D) multilayer films are suitable candidates for the current TCs. Recent investigation show that D/M/D structures such as indium tin oxide (ITO)/Au/ITO [13,14], titanium dioxide (TiO_2)/Au/TiO_2[15], zinc sulfide (ZnS)/Ag/ZnS [16] and zinc oxide (ZnO)/Au/ZnS/Au [17] have received much attention because of their high electrical and optical properties. For example, these structures show a very low sheet resistance at room temperature as well as a selective high transparent effect by suppressing the reflection from the metal layer. ZnS/Au/ZnS or ZAZ multilayer films in addition to low resistivity and high optical transmittance also have chemical and thermal stability. In addition, this multilayer structure system has not been studied so far. Structural, electrical and optical properties of the ZAZ films depend on various parameters such as: layer thickness, deposition rate, substrate and also the annealing temperature; therefore, exact optimization of above deposition parameters is necessary for the construction of the device. Among these parameters, the annealing temperature is one of the most important factors for determining of the electrical resistivity, optical and structural properties of ZAZ multilayer films. In this study, we have designed an optimum layer thickness of ZAZ multilayer structure and then prepared the ZAZ multilayer films by thermal evaporation. The effects of the annealing temperature on the properties of the ZAZ multilayer films were investigated. Comparison of the structural, electrical and optical properties of the ZAZ films as-deposited and after annealing was also carried out. X-ray diffraction (XRD), scanning electron microscopy (SEM) images, electrical resistivity and optical transmittance of the samples have been measured for this investigation.

* Corresponding author. Tel.: +98 3518122773; fax: +983518200132.
E-mail address: abehjat@yazduni.ac.ir (A. Behjat).

0169-4332/$ – see front matter © 2010 Elsevier B.V. All rights reserved.
doi:10.1016/j.apsusc.2010.08.103

2. Theory

2.1. The structural design of the transparent conductive multilayer films (optimization of the optical performance)

Optical performance of the design is calculated according to the characteristic matrix theory [10,18]. The transmittance, reflection and absorption of the multilayer film system were calculated and optimized.

2.2. Effects of ZnS and Au layers thickness on transmittance

A systematic study was carried out in order to determine the effect of each layer on the optical properties of ZnS/Au/ZnS films. The film arrangement was: air ($n_0 = 1, k_0 = 0$)/ZnS ($n_1, k_1 = 0$)/Au (n_2, k_2)/ ZnS(n_3, $k_3 = 0$)/glass ($n_4 = 1.56$, $k_4 = 0$), where n and k are the refractive index and extinction coefficient, respectively. The optical constants (n and k) in the wavelength region from 300 to 2000 nm for Au and ZnS films were used [19]. The calculations (for D/M/D films on a glass) were performed for normal incidence transmittance (T) and reflectance (R) using the equations from Refs. [10,18]. The mathcad14 software was used in all calculations. For determination of metal thickness, the optical constants at wavelength 550 nm, $n_2 = 0.228$ and $k_2 = 2.977$ and $n_1 = n_3 = 3.365$ for gold and ZnS were used, respectively [19].

The metal layer with the thickness of $d_2 = 19$ nm was used. More realistic values for the gold layer thickness are considered to less than 20 nm [13,15,17]. Such films are semi-transparent with significant reflectance in the infrared region. In Fig. 1, the transmittance is plotted as a function of the top dielectric layer thickness d_1 for different values of the ratio, $f = (d_3/d_1)$ (where d_3 is the bottom dielectric layer thickness). It is apparent from Fig. 1, that for the maximum transmittance at the design wavelength, $f = 1.15$. Therefore, transmittance has its maximum where the thickness of the third layer d_3 is equal to $d_3 = 1.15d_1$. An ideal transparent conductive multilayer systems has $T_{VIS} = 1$ and $R_{IR} = R_{UV} = 1$. For an optimum

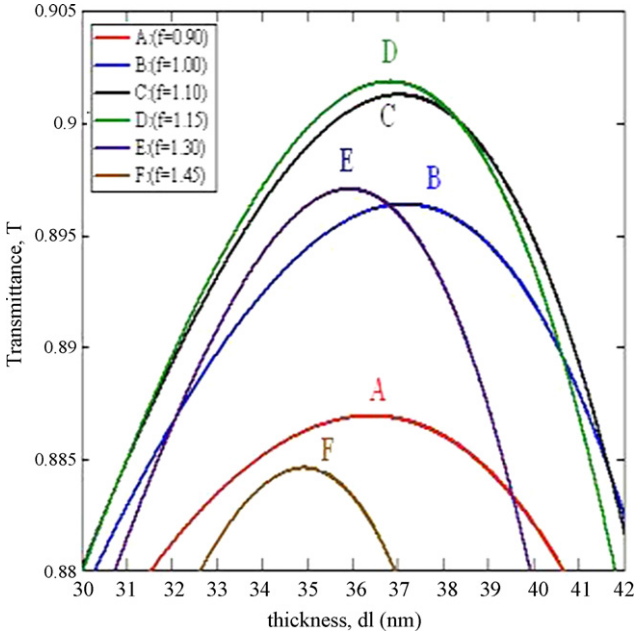

Fig. 1. Computer simulation for optimization of ZnS/Au/ZnS multilayers on a glass substrate. Effect of thickness (d_1 and d_3) of ZnS layers on transmittance at wavelength of 550 nm for different values of $f(= d_3/d_1)$.

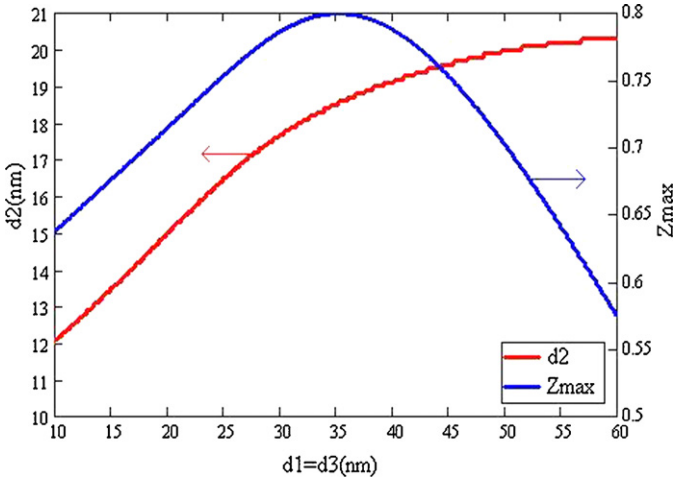

Fig. 2. The maximum Z factor and metal layer thickness, d_2, in compare with the first and third layer thickness.

performance of the system, the Z factor may be defined as:

$$Z = \left(\frac{\int T_{VIS}\,d\lambda}{\int d\lambda}\right)_{VIS}\left(\frac{\int R_{IR}\,d\lambda}{\int d\lambda}\right)_{IR}\left(\frac{\int R_{UV}\,d\lambda}{\int d\lambda}\right)_{UV} \quad (1)$$

similar to the previous work [2,3] where here the third term for UV is included.

For an ideal case, $T_{VIS} = R_{IR} = R_{UV} = 1$, Eq. (1) gives $Z = 1$. The thickness of the meal layer, d_2, optimized by using the Z factor along with the optical constants functions. In this way, the thickness of d_2 was calculated for different values of d_1, in a way that the maximum Z factor was obtained for this thickness. As a result, for the ZnS/Au/ZnS system, the Z factor is maximum when the Au-layer has a thickness of about 18.5 nm. As can be seen in Figs. 1 and 2 these optimum thicknesses for d_1, d_2 and d_3 are 35, 18.5 and 40 nm, respectively.

3. Experimental procedure

Thin films of ZnS/Au/ZnS nanostructures with the optimized structure of ZnS (35 nm)/Au (18.5 nm)/ZnS (40 nm) were deposited on a glass substrate by thermal evaporation. High purity polycrystalline ZnS and Au metal (99.99% purity) were used.

The glass substrates were cleaned sequentially by ultrasonication in propanol, acetone and deionized water for 10 min. Then the substrates were dried in a high purity N_2 gas stream just before they were loaded into the chamber. The substrate temperature during the deposition process was kept at room temperature.

The samples were located 14 cm above the molybdenum boat and rotated with the speed of 15 rpm in order to prepare uniform layer. The multilayer films successively deposited on a glass substrate without vacuum break, the chamber pressure bing 8×10^{-4} Pa. During the evaporation, layer thickness was monitored by a quartz crystal using an Edward FTM6 monitor. The evaporation rate of ZnS and Au were about 1 nm s^{-1}. The samples were annealed at 100, 200 and 300 °C for 60 min in air with heating rate of 5 K/min. The Philips 40 kV, 30 mA, Cu Kα X-ray diffraction measurements system with wavelength of 1.540598 nm in the scan range of 2θ between 10° and 90° with 0.05 (2θ s^{-1}) step size, were use for XRD studies.

Surface morphology of the films was observed by SEM. Sheet resistance of thin films was measured by a four point probe. The optical transmittance was measured in the range 200–1100 nm by a Cintra6 UV–Visible double-beam spectrophotometer.

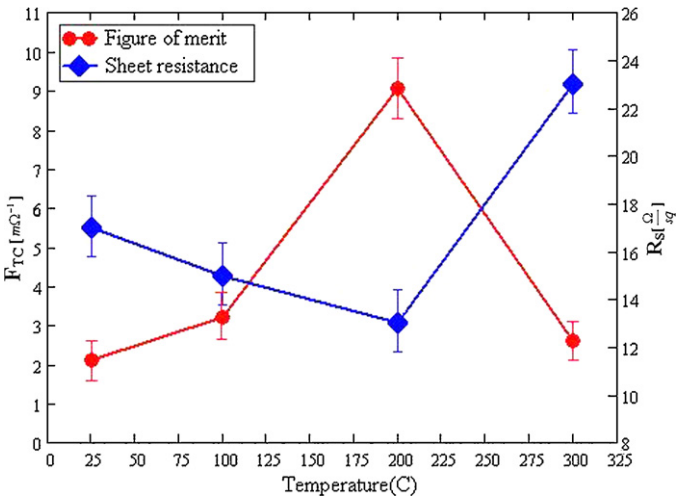

Fig. 3. The sheet resistance and figure of merit value of the ZAZ nano-multilayer samples as a function of annealing temperature.

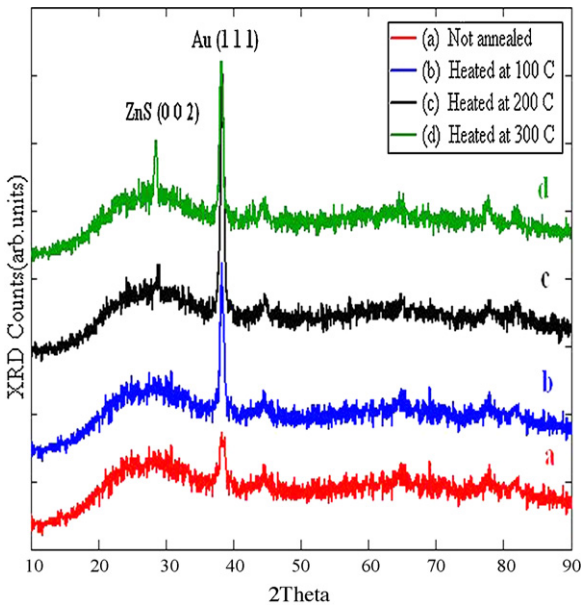

Fig. 4. XRD patterns of ZAZ nano-multilayer samples annealing at various temperatures.

4. Results and discussion

4.1. Electrical properties

In this study, optimum thickness of 18.5 nm Au layer in the design of the ZAZ multilayer structure is obtained (see Section 3). Remark that the sheet resistance is reciprocally proportional to the electron mobility and concentration. When the film thickness is large, there is a continuous Au film and holes among the linked islands are almost filled. Therefore, the electron mobility will increase and lead to decrease of the sheet resistance of the ZAZ multilayer films. Similar study for TiO_2/Au/TiO_2 structures with $d_{Au} = 8$ nm and $d_{TiO_2} = 55$ nm thickness is reported [15].

The resistivity of the samples were measured by the four-point probe method. Fig. 3 shows the change of resistivity of the ZAZ multilayer films as a function of the annealing temperature. It is observed that the resistivity is decreases slowly with the annealing temperature from 17 Ω/sq in as-deposited film at 25 °C and achieves a minimum value of 13 Ω/sq at 200 °C. The reduction of resistivity in this temperature range is due to the reduction of grain boundary scattering of multilayer system which is confirmed with X-ray diffraction patterns and SEM images that is shown in Figs. 4 and 5. However, significant increase of resistivity with increase in annealing temperature up to 300 °C can be observed. It seems that this is basically due to severe inter diffusion of atoms at the Au/ZnS interfaces. Where, Au atoms diffuse through ZnS layers and oxygen (O_2) atoms diffuse through Au layers, which cause the oxidation of the metal layers. Therefore, the sheet resistance increases at higher temperatures.

4.2. Structural properties

The crystalline structure of the ZAZ multilayer films as-deposited at room temperature and after annealing at different temperatures in air was investigated by XRD. The results are shown in Fig. 4. It can be seen that before heat treatment, the films are approximately amorphous. The diffraction peak at $2\theta = 38.269°$ is contributed by Au (1 1 1). The JCPDS card shows that $2\theta = 28.68°$ corresponds to both ZnS (0 0 2) with hexagonal structure and ZnS with (1 1 1) cubic structure diffraction peaks. Prathap et al. [20], reported the hexagonal structure for 100 nm thick ZnS films and cubic structure for the films with thickness of more than 300 nm. Therefore, the diffraction pattern could not determine the exact structure of the ZnS films. Moreover, one can observe that gold film has (1 1 1) predominant orientation in the process of growth. The peaks intensities are increased by increasing annealing temperature.

The influence of annealing temperature on grain size of Au in the ZAZ multilayer films was also investigated. The grain size (G) was calculated using the Scherrer equation [21]:

$$G = \frac{K\lambda}{\beta \cos\theta}, \quad (2)$$

where K denotes the Scherrer constant ($K = 0.89$) [22], λ is the wavelength of the Cu Kα radiation ($\lambda = 1.54056$ nm) and β is the full width at half maximum (FWHM) of a Gaussian fit. The values for the FWHM and the center of the peak (θ), calculated using the Gaussian fit, for the samples are listed in Table 1. It can be seen that the grain size of Au increases with increasing the annealing temperature and as a result crystallinity of samples improves.

Fig. 5 shows the SEM surface topography of the ZAZ multilayer films for as- deposited and annealed samples at 100, 200 and 300 °C, respectively. It is found that the surface morphology of the as-deposited ZAZ films is less uniform and with increasing annealing temperature the grain size becomes larger and structural homogeneity of films improves that this result agrees with the XRD analysis. For similar systems (such as: ZnS/Ag/ZnS, ITO/Ag,Cu/ITO, ZnO/Au/ZnS/Au) this behavior also has been observed [17,23,24].

4.3. Optical transmittance

The optical transmittance spectra of the ZAZ multilayer films coated on glass substrates as a function of the annealing temperature, in the range from 350 to 1100 nm were measured and are presented in Fig. 6. As can be observed, transmission of the ZAZ films are changed from 72% to 81% for as-deposited and annealed sample at 200 °C, respectively. This behavior can be attributed to the enhancement of Au layer crystallinity which result is in coincidence with SEM images. Then, by further increasing of annealing temperature up to 300 °C, the optical transmission decreases to 74%. It seems that this result is due to surface roughening of Au layer during annealing and diffusion of Au atoms into ZnS layer results in more scattering of the incident light and reduction of the transmittance.

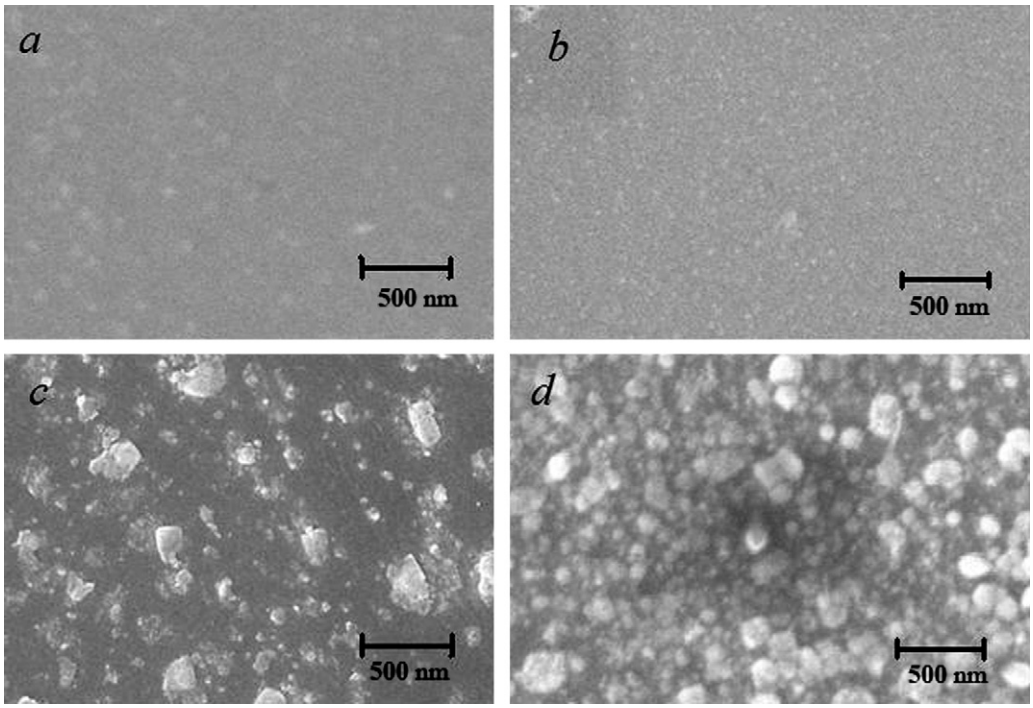

Fig. 5. SEM images of the ZAZ nano-multilayer films at different annealing temperature (a: as-deposited, b: 100 °C, c: 200 °C and d: 300 °C).

Table 1
The electrical, structural and optical properties of ZAZ multilayer films with various annealing temperatures.

Deposition temperature [°C]	Sheet resistance [±1 Ω/sq]	2θ(°)	β(°)	Particle size [nm]	Transmittance [% at 550 mm]	Average transmittance [%]	F_TC [m Ω^{-1}]
As-deposited	17	–	–	–	71.7	66.5	2.1±0.3
100	15	38.22	0.48	17±2	73.8	66.0	3.2±0.5
200	13	38.31	0.24	34±5	80.7	72.4	9.0±0.6
300	23	38.17	0.48	17±2	75.5	66.6	2.6±0.3

The *figure of merit* (F_{TC}) is important factor that represents briefly the relationship between electrical and optical properties of transparent conducting films. This factor which is used for comparing the performance of ZAZ multilayer films annealed in different temperatures, the F_{TC} is defined as [25]:

$$F_{TC} = \frac{T^{10}}{R_S} \quad (3)$$

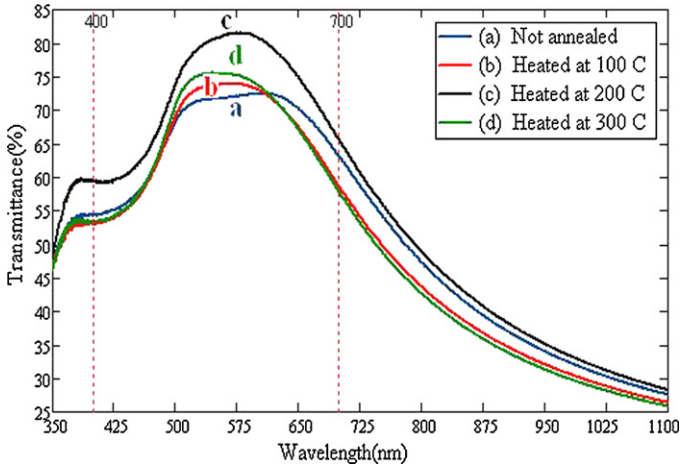

Fig. 6. Optical transmission spectra of the ZAZ nano-multilayer films at various annealing temperature (a: as-deposited, b: 100 °C, c: 200 °C and d: 300 °C).

where T is the transmittance of multilayer at 550 nm wavelength and R_S is the sheet resistance of transparent conducting system. Fig. 3 shows variation of the figure of merit versus the annealing temperature, the F_{TC} value increases by increasing the annealing temperature, and maximum F_{TC} value of the ZAZ multilayer films can be obtained at 200 °C. Further increases of annealing temperature, however, led to a decrease in F_{TC} value. Therefore, the ZAZ multilayer film annealed in 200 °C temperature is a promising structure for this transparent conducting system.

5. Summary and conclusion

The ZnS/Au/ZnS nano-multilayer films were prepared on glass at room temperature. The samples were annealed in air at different temperatures from 100 to 300 °C for an hour to investigate the effect of annealing treatment on the structural, electrical and optical properties of the samples. The sheet resistance decreases slowly with the increase in the annealing temperature and achieves a minimum value at 200 °C. A significant increase in sheet resistance occurs by increasing the annealing temperature to 300 °C. Furthermore, the XRD patterns show that crystalinity of the samples improves as a result of annealing. Optical transmittance increases by heat treatment and at 200 °C, reaches to 81% and then decreases to 74% by increasing the temperature up to 300 °C. The SEM images show that the grain size becomes larger by increasing the annealing temperature and this result agrees with result from the XRD analysis. In brief, the annealing temperature has an important role in controlling the electrical,

optical and structural properties of the nanostructured multilayer films.

Acknowledgments

The support of the Ministry of Energy for this project is gratefully acknowledged. Authors also wish to thank the photonics group of the Physics Department, Yazd University for their Laboratory support.

References

[1] D. Song, A.G. Aberle, J. Xia, Appl. Surf. Sci. 195 (2002) 291.
[2] A.M. Al-Shukri, Desalination 209 (2007) 290.
[3] S.M.A. Durrani, E.E. Khawaja, A.M. Al-Shukri, M.F. Al-Kuhaili, Energy Build. 36 (2004) 891.
[4] T. Schuler, M.A. Aegerter, Thin Solid Films 351 (1999) 125.
[5] K.L. Chopra, S. Major, K. Pandya, Thin Solid Films 102 (1983) 1.
[6] G. Claes, Granqvist, Solar Energy Mater. Solar Cells 91 (2007) 1529.
[7] K. Matsubara, P. Fons, K. Iwata, A. Yamada, K. Sakurai, H. Tampo, S. Niki, Thin Solid Films 431/432 (2003) 369.
[8] Y.C. Lin, S.J. Chang, Y.K. Su, C.S. Chang, S.C. Shei, J.C. Ke, H.M. Lo, S.C. Chen, C.W. Kuo, Solid-State Electron. 47 (2003) 1565.
[9] G. Leftheriotis, S. Papaefthimiou, P. Yianoulis, Solid State Ionics 136–137 (2000) 655.
[10] X. Liu, X. Cai, J. Qiao, J. Mao, N. Jiang, Thin Solid Films 441 (2003) 200.
[11] G.J. Fang, D. Li, B.L. Yao, Thin Solid Films 418 (2002) 156.
[12] D.H. Zhang, T.L. Yang, J. Ma, Appl. Surf. Sci. 158 (2000) 43.
[13] Y.S. Kim, J.H. Park, D.H. Choi, H.S. Jang, J.H. Lee, H.J. Park, J.I. Choi, D.H. Ju, J.Y. Lee, D. Kim, Appl. Surf. Sci. 254 (2007) 1524.
[14] D. Kim, Appl. Surf. Sci. 256 (2010) 1774.
[15] P.C. Lansker, J. Backholm, G.A. Niklasson, C.G. Granqvist, Thin Solid Films 518 (2009) 1225.
[16] X. Liu, X. Cai, J. Mao, C. Jin, Appl. Surf. Sci. 183 (2001) 103.
[17] E. Turan, M. Zor, A. Senol Aybek, M. Kul, Thin Solid Films (2009) 8752.
[18] H.A. Macleod, Thin Film Optical Filters, 3rd edition, Institute of Physics publishing, 2001.
[19] D. Edward, Palik, Handbook of Optical Constant of Solid, Academic Press, USA, 1998.
[20] P. Prathap, N. Revathi, Y.P. Venkata Subbaiah, K.T. Ramakrishna Reddy, J. Phys. Condens. Matter (2008) 20.
[21] B.D. Cullity, Elements of X-Ray Diffraction, 2nd edition, Addison-Wesley, MA, 1978 (Chapter 9).
[22] M. Abdullah, Khairurrijal, J. Nano Saintek 1 (2008) 28.
[23] P. Zhao, W. Su, R. Wang, X. Xu, F. Zhang, Physica E 41 (2009) 387.
[24] C. Guillen, J. Herrero, Solar Energy Mater. Solar Cells 92 (2008) 938.
[25] G. Haacke, J. Appl. Phys. 47 (1976) 4086.